

Loss of SMEK, a Novel, Conserved Protein, Suppresses *mek1* Null Cell Polarity, Chemotaxis, and Gene Expression Defects

Michelle C. Mendoza,^{1,2} Fei Du,¹ Negin Iranfar,¹ Nan Tang,^{1†} Hui Ma,^{1‡}
William F. Loomis,¹ and Richard A. Firtel^{1*}

Section of Cell and Developmental Biology, Division of Biological Sciences, Center for Molecular Genetics, University of California, San Diego, 9500 Gilman Drive, La Jolla, California 92093-0380,¹ and Biomedical Sciences Graduate Program, School of Medicine, University of California, San Diego, 9500 Gilman Drive, La Jolla, California 92093²

Received 25 January 2005/Returned for modification 15 March 2005/Accepted 3 June 2005

MEK/extracellular signal-regulated kinase (ERK) mitogen-activated protein kinase signaling is imperative for proper chemotaxis. *Dictyostelium mek1*⁻ (MEK1 null) and *erk1*⁻ cells exhibit severe defects in cell polarization and directional movement, but the molecules responsible for the *mek1*⁻ and *erk1*⁻ chemotaxis defects are unknown. Here, we describe a novel, evolutionarily conserved gene and protein (*smkA* and SMEK, respectively), whose loss partially suppresses the *mek1*⁻ chemotaxis phenotypes. SMEK also has MEK1-independent functions: SMEK, but not MEK1, is required for proper cytokinesis during vegetative growth, timely exit from the mound stage during development, and myosin II assembly. SMEK localizes to the cell cortex through an EVH1 domain at its N terminus during vegetative growth. At the onset of development, SMEK translocates to the nucleus via a nuclear localization signal (NLS) at its C terminus. The importance of SMEK's nuclear localization is demonstrated by our findings that a mutant lacking the EVH1 domain complements SMEK deficiency, whereas a mutant lacking the NLS does not. Microarray analysis reveals that some genes are precociously expressed in *mek1*⁻ and *erk1*⁻ cells. The misexpression of some of these genes is suppressed in the *smkA* deletion. These data suggest that loss of MEK1/ERK1 signaling compromises gene expression and chemotaxis in a SMEK-dependent manner.

Chemotaxis is a conserved cellular process in which cells detect a chemical gradient, polarize, and proceed up the gradient by extending a pseudopod at their leading edge and retracting their posteriors (17, 27, 40). In both mammalian and *Dictyostelium* cells, mitogen-activated protein (MAP) kinase pathways are required for proper chemotaxis. Mouse knockout studies have shown that MEKK1, a MAP kinase kinase that scaffolds and activates both the extracellular signal-regulated kinase (ERK) ERK1/2 and stress-activated Jun N-terminal protein kinase (JNK) MAP kinase pathways, is required for epithelial and fibroblast migration (65). Fibroblasts from *mek1*^{-/-} (MEK1 is a MAP kinase kinase that specifically activates ERK1/2) and *jnk1*^{-/-}*jnk2*^{-/-} mice also exhibit reduced directional motility in fibronectin and wound-induced migration assays (20, 25). In addition, ERK1/2 activation is required for MDCK epithelial cells moving as a sheet or undergoing a partial epithelial-to-mesenchymal transition during tubulogenesis (36, 39).

One MEK and two ERK family MAP kinases have been identified in *Dictyostelium*. Cells lacking MEK1 or ERK1 (*mek1*⁻ and *erk1*⁻ cells) exhibit a marked absence of polarity and severely reduced chemotaxis speed and directionality (34,

50). *Dictyostelium* MEK1 is required for ERK1 activation and its localization to the cell cortex in response to chemoattractant stimulation (50). ERK2 is not regulated by MEK1 but has an established role in phosphorylating the RegA phosphodiesterase during starvation-induced cyclic AMP (cAMP) relay signaling (35).

Although the ERK and JNK MAP kinase pathways are required for cell motility in many systems, their critical downstream effectors during amoeboid chemotaxis have not been identified. Traditionally, the MAP kinases have been modeled in linear pathways in which signals from receptors at the cell surface cause phosphorylation of the activating MEK kinases and MEKs (MAP kinase kinases), followed by phosphorylation of the MAP kinases and their translocation to the nucleus (21, 42). In the nucleus, MAP kinases activate transcription factors responsible for the expression of immediate-early genes (21). The kinases are inactivated by dephosphorylation of a threonine and tyrosine in their activation loop before they exit to the cytoplasm (58). However, activated ERK has also been found in the extending pseudopodia of migrating fibroblasts, in the focal adhesions and spreading lamellipodia of newly adherent fibroblasts, and in the cytoplasm of epithelial cells at the front of migrating sheets (4, 15, 28, 36).

Studies with fibroblasts and epithelial cells indicate that ERK's function at the leading edge is to phosphorylate and activate the myosin II motor and specific focal adhesion proteins. Myosin light-chain (MLC) kinase (MLCK) phosphorylation of MLC activates myosin motor activity (11). In vitro, ERK1 can directly phosphorylate and activate MLCK (28). Pharmacological inhibition of either MEK or MLCK in

* Corresponding author. Mailing address: Natural Science Building, Room 6316, University of California, San Diego, 9500 Gilman Drive, La Jolla, CA 92093-0380. Phone: (858) 534-2788. Fax: (858) 822-5900. E-mail: rafirtel@ucsd.edu.

† Present address: Molecular Pathology Graduate Program, University of California, San Diego, 9500 Gilman Drive, La Jolla, CA 92093.

‡ Present address: Salk Institute for Biological Sciences, 10010 North Torrey Pines Road, La Jolla, CA 92037.

spreading fibroblasts reduces focal adhesion disassembly, and inhibition of MEK in immortalized kidney cells reduces MLCK activity and MLC phosphorylation (7, 60). However, functional MLCK is required for ERK1 localization to focal adhesions (15), indicating that MEK/ERK signaling and MLCK have a more complex relationship than a simple linear pathway. ERK also interacts with the focal adhesion protein paxillin in a multifaceted manner. Paxillin is an adaptor protein that can recruit ERK to focal adhesions, ERK and JNK can phosphorylate paxillin, and paxillin phosphorylation potentiates epithelial cell spreading and motility (6, 23, 31).

The function of MEK1/ERK1 signaling during amoeboid chemotaxis, such as that seen in leukocytes, metastatic cancer cells, and *Dictyostelium*, has not been studied as thoroughly. This type of cell movement is more rapid and does not involve focal adhesions (17). In *Dictyostelium*, active myosin II is located along the cortex of the posterior two-thirds of moving cells (the myosin motor retracts the posterior, and assembled filaments provide structural support to prevent aberrant lateral pseudopod extension), not in the extending pseudopodia (11, 27, 40). Loss of *Dictyostelium* MLC results in severe cytokinesis, morphogenesis, and motility defects, but mutation of the activating MLC phosphorylation sites causes only an increase in chemotaxis speed and decrease in lateral pseudopod extension (it has no effect on cytokinesis or morphogenesis). Loss of the *Dictyostelium* MLC activator, MLCK-A, causes a conditional cytokinesis defect during growth in shaking culture but no chemotaxis phenotype (12). Thus, ERK1 phosphorylation of MLCK is unlikely to fully explain why MEK1/ERK1 signaling is so essential to amoeboid chemotaxis.

To better understand which molecules are responsible for the *mek1*⁻ and *erk1*⁻ cell polarization and motility defects, we screened for second-site suppressors of the *mek1*⁻ small-mound phenotype in *Dictyostelium* cells. We discovered a novel, highly conserved gene, *smkA* (for suppressor of *mek1*⁻), that is required for the chemotaxis defects of *mek1*⁻ cells. Independent of MEK1, loss of SMEK causes cytokinesis and developmental phenotypes similar to those of cells with reduced cortical tension (12, 13, 44). Also independent of the MEK1/ERK1 pathway, SMEK overexpression severely reduces cell polarization and chemotaxis.

We find that SMEK function is regulated by its localization. SMEK localizes to the cell cortex in vegetative cells but translocates to the nucleus during starvation and development. A SMEK mutant lacking the conserved nuclear localization signal (NLS) constitutively localizes to the cell cortex and is unable to complement *smkA*⁻ deficiency, demonstrating that SMEK nuclear localization is necessary for its function. Microarray analysis determined that some late genes are precociously expressed in *mek1*⁻ and *erk1*⁻ cells. Loss of SMEK suppresses this misexpression for several of these genes, indicating that their precocious expression requires the presence of SMEK. Thus, this novel, conserved protein causes some of the *mek1*⁻ defects in cell polarization, chemotaxis, and gene expression in *Dictyostelium*.

MATERIALS AND METHODS

REMI screen and cloning of SMEK. We created a *mek1*⁻ mutant of the thymidine-requiring JH10 strain. For the restriction enzyme-mediated integration (REMI) screen, log-phase *mek1*⁻ JH10 cells were electroporated with a

REMI vector containing the blasticidin resistance cassette and the restriction enzyme DpnII. Transformants were selected in 10 µg/ml blasticidin and plated on SM agar with *Klebsiella aerogenes*. Colonies with wild-type-sized mounds and slugs were harvested, and genomic DNA sequences flanking the insertion sites were cloned and used as probes for Southern blot analysis as described previously (32, 46). SMEK¹⁻⁸¹¹ was obtained by screening λZAP cDNA and genomic libraries with a probe amplified from genomic DNA by PCR. The C terminus was obtained by PCR amplification from *Dictyostelium* strain KAx-3 genomic DNA with primers based on the predicted *smkA* gene sequence (DDB0188242) in the *Dictyostelium* Genome Project database (<http://dicty.sdsc.edu>). In-frame PCR was used to add the N-terminal hemagglutinin (HA) tag and create the EVH1 and NLS deletion mutants. All constructs were ligated into the EXP-4(+) expression vector.

Independent knockout and overexpression SMEK cell lines. *Dictyostelium* cells were grown in axenic HL5 medium and transformed by electroporation. The KAx-3 strain was used to generate the *smkA*⁻ and SMEK-overexpressing cell lines. The *mek1*⁻ JH10 strain was used to generate the *mek1*⁻/*smkA*⁻ cell line. To knock out SMEK, a HindIII/BamHI linker and the blasticidin resistance BSr gene cassette were inserted after the first 300 bp of the *smkA* coding sequence. For overexpression of SMEK, cells were selected in the presence of G418 (20 µg/ml) as described previously (19). Clones were screened by immunoblotting to identify those expressing high and low levels of exogenous SMEK.

Development and chemotaxis analysis. Developmental morphology was observed by plating washed log-phase cells on nonnutrient agar plates (34). Chemotaxis in response to cAMP gradient stimulation was examined as described previously (9, 19). Briefly, cells were pulsed with 30 nM cAMP at 6-min intervals for 5 h and plated on glass-bottomed microwell plates. A micropipette containing 150 µM cAMP was positioned to stimulate the cells, using a micromanipulator (Eppendorf-Netheler-Hinz GmbH), and the response of the cells was recorded using a time-lapse video recorder and NIH Image software (one image every 6 s). Computer-assisted analysis of cell movement and shape change was performed using the DIAS program (61).

Isolation of cytoskeletal myosin II. Cells were starved for 2 h, pulsed with 100 nM cAMP for 5 h, and treated with 1 mM caffeine for 30 min before stimulation with 100 µM cAMP. Cytoskeletal proteins were isolated as proteins insoluble in the detergent Triton X-100 as described previously (53). The protein pellets were dissolved by being boiled in 2× sodium dodecyl sulfate-polyacrylamide gel electrophoresis sample buffer, run on 7.5% acrylamide gels, and stained with Coomassie blue. Protein bands were scanned and changes in myosin II content were quantitated using Image Gauge software.

Indirect immunofluorescence staining. For immunofluorescence staining, vegetative cells were taken from shaking culture and allowed to adhere to coverslips. For chemotaxis analysis, cells were pulsed with 30 nM cAMP at 6-min intervals for 5 h in 12 mM sodium phosphate buffer (pH 6.2). Cells were allowed to adhere to and begin chemotaxing on the coverslips or were stimulated with 150 µM cAMP before fixation in -20°C ethanol and 1% formaldehyde. Cells were permeabilized with 0.5% Triton X-100, washed, and incubated with 10 mg/ml mouse anti-HA antibody (Covance) in phosphate-buffered saline containing 0.5% fetal bovine serum and 0.05% Tween 20 overnight at 4°C. Cells were washed in 0.5% fetal bovine serum in phosphate-buffered saline and incubated with tetramethyl rhodamine isocyanate-conjugated anti-mouse (Molecular Probes) or fluorescein isothiocyanate-conjugated anti-rabbit (Southern Biotechnology) antibodies for 1 h. F-actin was stained with rhodamine-conjugated phalloidin (Sigma). We acquired images with either a confocal or a DeltaVision deconvolution microscope system.

RNA preparation and cDNA microarray analysis. Cells (10⁷ cells/ml) were starved in Na-K phosphate buffer for 1 h, pulsed with 30 nM cAMP every 6 min for 5 h, and then stimulated once with 300 µM cAMP. RNA was prepared from 5 × 10⁷ cells every 2 h by dissolving in Trizol reagent (Gibco/BRL). Reference RNA was prepared by pooling samples collected throughout development. Probes were prepared, hybridized to microarrays, and analyzed as described previously (24). Briefly, Superscript II DNA polymerase (Invitrogen) was used to incorporate either Cy5 or Cy3-conjugated dCTP (Amersham) into DNA, using constant amounts of RNA as template. After removal of the unincorporated dyes (Millipore), the probes were mixed and hybridized to the microarrays for 6 to 12 h. The microarrays carried unique 50-bp oligonucleotides for the 600 genes (<http://www.biology.ucsd.edu/loomis/cgi/microarray/Smek-array.html>). Dyes for the sample and reference probes were interchanged in different experiments. Probed microarrays were analyzed in an Axon Genepix 4000B scanner. Total Cy3 signal was normalized to total Cy5 signal after background subtraction, and the Cy3/Cy5 ratio was calculated for individual genes. Each developmental time course was repeated at least twice. Mean values were used for subsequent

analysis. Protocols are available at <http://www.biology.ucsd.edu/loomis-gi/microarray/index.html>.

RESULTS

Identification of *smkA*. During *Dictyostelium* development, cell-cell communications and intracellular signaling events are coordinated with cell movement towards cAMP to result in the formation of multicellular aggregates (mounds) that undergo morphogenesis to form a mature fruiting body (8). *Dictyostelium* cells lacking MEK1 or ERK1 form extremely small developmental aggregates due to their impaired chemotaxis (34, 50). To discover the proteins responsible for the *mek1*⁻ defective chemotaxis, we performed a second-site suppressor screen of the *mek1*⁻ aggregation phenotype by using REMI mutagenesis. REMI randomly inserts a plasmid sequence in the genome and usually yields a null mutation (46). We identified a novel gene, *smkA*, which is required for the *mek1*⁻ developmental phenotype (loss of SMEK in a *mek1*⁻ background partially suppresses the *mek1*⁻ phenotypes) (Fig. 1A). Northern blotting of the *Dictyostelium smkA* transcript shows that *smkA* mRNA levels are constant throughout development (data not shown).

A BLAST search of GenBank identified highly conserved SMEK homologs in organisms ranging from yeast to humans (Fig. 1B and C). BLAST searches of the iGAP database, which uses fold recognition and threading rather than simple sequence identity (33), identified a putative EVH1 domain at the N terminus. EVH1 domains are sequences of 110 amino acids that bind to proline-rich regions in a variety of binding partners (22). There is 72% similarity between the EVH1 domain of the *Dictyostelium* SMEK protein and that of the two human homologs. The domain also contains a highly conserved tyrosine and tryptophan that align with the central Y16 and W22 (human VASP numbering) found in type I EVH1 domains (Fig. 1B and C). A central domain of undetermined function (PFAM DUF625) exhibits 60% similarity between *Dictyostelium* and human SMEKs (Fig. 1B). Although much of the *Dictyostelium* SMEK C terminus is simple sequence and unconserved, it contains a conserved stretch of acidic residues followed by basic residues (Fig. 1B and C).

SMEK function is required for *mek1*⁻ cell polarity and chemotaxis defects. We independently generated *smkA*⁻ and *mek1*⁻/*smkA*⁻ knockout strains by using homologous recombination (see Materials and Methods). Random transformants were selected and screened for disruption of *smkA* by Southern and Northern blot analyses (data not shown). Several independently derived single and double mutant strains were examined; all in each class exhibited the same developmental and chemotaxis phenotypes (data not shown). We used single representative *smkA*⁻ and *mek1*⁻/*smkA*⁻ clones for subsequent studies.

Wild-type cells form a multicellular organism through a starvation-induced developmental program. After ~9 h of starvation, the chemotactic aggregation of up to 10⁵ cells leads to the formation of multicellular mounds. Morphogenesis ensues, with the formation of an apical tip after ~12 h. The organism elongates and forms a migrating pseudoplasmodium (slug) between 14 and 16 h and initiates culmination to form a mature fruiting body at ~20 h of development (Fig. 2A) (7). Forma-

tion of a mound can be used as a read-out of successful aggregation and the tipped aggregate as a read-out of the initiation of morphogenesis (3, 27). *smkA*⁻ cells resemble wild-type cells in their ability to aggregate and form mounds (Fig. 2A, 9 h; Table 1). In contrast, *mek1*⁻ cells form tiny mounds, and morphogenesis is more rapid than in wild-type strains (pseudoplasmodia are formed by 12 h, and fruiting body formation initiates by 16 h). *mek1*⁻/*smkA*⁻ cells resemble wild-type cells in their ability to aggregate but form mounds that are intermediate in size between those of *mek1*⁻ cells and wild-type cells (Fig. 2A, 9 h; Table 1; data not shown). The developmental timing of *mek1*⁻/*smkA*⁻ cells is also similar to that of wild-type cells (Fig. 2A, 16 and 24 h). Thus, SMEK is required for the mound size and precocious developmental defects of *mek1*⁻ cells.

To confirm that loss of SMEK was the cause of the observed *smkA*⁻ phenotypes, we cloned and expressed HA-tagged full-length SMEK from the Act15 promoter in *smkA*⁻ and *mek1*⁻/*smkA*⁻ cells (*smkA*⁻/SMEK^{OE} and *mek1*⁻/*smkA*⁻/SMEK^{OE}). Expression of SMEK was verified by anti-HA immunoblotting (data not shown). Overexpression of HA-SMEK complements *smkA*⁻ mound stage defects and reverts *mek1*⁻/*smkA*⁻ cells to the *mek1*⁻ phenotype. However, many *smkA*⁻/SMEK^{OE} and *mek1*⁻/*smkA*⁻/SMEK^{OE} cells do not enter the developing mounds (Fig. 2A; Table 1; see Fig. 6A). This phenotype was also observed in wild-type cells overexpressing HA-SMEK (KAX-3/SMEK^{OE}) and is attributed to the high levels of SMEK protein caused by overexpression.

We next determined if SMEK is required for *mek1*⁻ defects in cell polarity and chemotaxis, which contribute to the *mek1*⁻ small-mound phenotype. We analyzed the polarity, directionality, and speed of individual *mek1*⁻/*smkA*⁻ cells chemotaxing up a cAMP gradient. As shown in Fig. 2B and quantified in Table 2, *mek1*⁻/*smkA*⁻ cells exhibit dramatically improved chemotaxis profiles compared to those of *mek1*⁻ cells (48% roundness in *mek1*⁻/*smkA*⁻ cells, 73% in *mek1*⁻ cell, and 47% in reference wild-type KAX-3 cells) (Table 2). A similar improvement is seen in their directionality. Furthermore, *mek1*⁻/*smkA*⁻ cells move >2-fold faster than *mek1*⁻ cells, at a speed that is comparable to that of wild-type cells (10 μm/min for *mek1*⁻/*smek*⁻ cells, compared to ~3 μm/min for *mek1*⁻ and ~11 μm/min for KAX-3 cells) (Table 2). Loss of SMEK in a wild-type background causes a mild increase in the frequency of direction change and slowing of chemotaxis, similar to the levels observed in the *mek1*⁻/*smkA*⁻ strain. Thus, *smkA*⁻ partially suppresses *mek1*⁻ defects in mound size during aggregation, and it completely suppresses the *mek1*⁻ cell polarity and chemotaxis defects (Tables 1 and 2).

Loss of SMEK causes reduced chemoattractant-mediated myosin assembly. We noted that loss of SMEK in both wild-type and *mek1*⁻ backgrounds causes a delay in exit from the mound stage and a mild increase in lateral pseudopod production (Fig. 2A and B). *smkA*⁻ cells do not reach the slug stage until 24 h of development and form morphologically abnormal fruiting bodies after 36 h (Fig. 2A, 36 h). *mek1*⁻/*smkA*⁻ cells form slugs at the same time as wild-type cells (16 h), but are delayed in comparison to *mek1*⁻ cells, and form aberrant fruiting bodies at 24 h (Fig. 2A, 16 and 24 h). Myosin II provides structural support (cortical tension) along the sides of chemotaxing cells to prevent such aberrant lateral pseudopod extension and support during the formation of a mound tip that

eventually falls over to become a slug (11, 27, 40). Importantly, *Dictyostelium* cells lacking myosin II, expressing dominant negative myosin II, or overexpressing myosin heavy chain kinase do not develop past the mound stage (13, 29, 55). Therefore, we assayed the *smkA*⁻ and *mek1*⁻/*smkA*⁻ strains for growth defects known to result from reduced myosin II activity.

Cells with inactive or no myosin II also have a conditional cytokinesis defect (12, 13, 44). These strains exhibit little increase in cell number when grown in suspension culture but are able to divide and proliferate on a substratum via traction-mediated cytofission. Both *smkA*⁻ and *mek1*⁻/*smkA*⁻ cells exhibit such a conditional cytokinesis defect (Fig. 3A). When grown in suspension culture, the cells form abnormally large, multinucleate structures, but the cells are predominantly mononucleate on a substratum (Fig. 3A). These data show that in addition to mediating the *mek1*⁻ chemotaxis defects, SMEK plays a MEK1-independent role in exit from the mound stage and cytokinesis.

Because *smkA*⁻ and *mek1*⁻/*smkA*⁻ cells exhibit phenotypes similar to those of strains that are defective in myosin II assembly (lateral pseudopod extension during chemotaxis, mound arrest, and cytokinesis defects in suspension), we hypothesized that SMEK was required for proper myosin II localization or assembly. We examined the subcellular distribution of myosin II during chemotaxis by using green fluorescent protein-myosin II, which retains wild-type localization and catalytic activity (38). The green fluorescent protein-myosin II reporter properly localizes to the posterior of chemotaxing *smkA*⁻ cells and the cleavage furrow of dividing *smkA*⁻ cells, indicating that SMEK is not required for proper localization of either component (data not shown).

We assayed the ability of *smkA*⁻ cells to assemble myosin II in response to chemoattractant stimulation by isolating Triton-insoluble cytoskeletal fractions from cells stimulated with cAMP for different lengths of time (41, 53). In the basal (unstimulated) state, the amount of myosin II in the total cell protein of *mek1*⁻ cells is 90% of that of wild-type cells. *mek1*⁻ cells exhibit a wild-type myosin II response pattern following chemoattractant stimulation. This profile is characterized by a 3.0- to 3.3-fold increase in myosin II in the cytoskeletal fraction that peaks at between 30 and 50 s poststimulation (Fig. 3B) (41, 53). In contrast, *smkA*⁻ and *mek1*⁻/*smkA*⁻ cells exhibit elevated basal levels of assembled myosin II (both 120% of the wild-type level) but reduced accumulation of myosin II in the Triton-insoluble fraction after stimulation with cAMP, compared to wild-type cells (Fig. 3B). *smkA*⁻ cells display only a 1.9-fold induction and *mek1*⁻/*smkA*⁻ cells a 2.1-fold induction of assembled myosin II. These data are consistent with the

observation of *myosin II*⁻-like phenotypes in *smkA*⁻ and *mek1*⁻/*smkA*⁻ cells and suggest that independent of MEK1, SMEK can influence proper myosin II assembly (13, 54, 62).

SMEK overexpression in wild-type and *mek1*⁻ cells causes reduced cell polarity and chemotaxis. Next, we determined whether SMEK overexpression affects cell polarization and chemotaxis. When KAx-3/SMEK^{OE} cells undergo developmental morphogenesis, most of the cells fail to join the aggregates, and the mounds and fruiting bodies that do form take longer to develop and are smaller than wild type (Fig. 2A). Furthermore, cells with very high levels of SMEK are likely selected against during growth, since the strain grows more slowly than wild-type cells (data not shown). SMEK overexpression in the *mek1*⁻ and *erk1*⁻ backgrounds causes slow aggregation (Fig. 2A and data not shown), indicating that the SMEK overexpression phenotype does not require the presence of MEK1 or ERK1 and is thus independent of the MEK1/ERK1 pathway. Wild-type cells overexpressing full-length HA-tagged SMEK (KAx-3/SMEK^{OE}) are round and unpolarized (76% roundness) (Fig. 2B; Tables 1 and 2). KAx-3/SMEK^{OE} cells exhibit little directionality during chemotaxis (0.17) and move slowly (3.5 μm/min) (Table 2). Thus, proper SMEK expression levels are critical for effective cell polarity and chemotaxis.

SMEK subcellular localization is regulated between the cell cortex and nuclear compartments. We determined the subcellular localization of SMEK by using indirect immunofluorescence. In vegetative cells, full-length HA-tagged SMEK localizes to the cell cortex (Fig. 4). After the cells are pulsed in Na-K phosphate buffer for 6 h to render them competent for chemotaxis, SMEK is in the nucleus. Because our identification of SMEK as a genetic suppressor of *mek1*⁻ suggests that SMEK could function downstream of MEK1, we tested whether the MEK1/ERK1 pathway controls SMEK localization. In both *mek1*⁻ and *erk1*⁻ cells, HA-SMEK exhibits the same pattern of subcellular localization as in wild-type cells (data not shown), indicating that SMEK localization is not regulated by MEK1/ERK1 signaling.

In *Dictyostelium*, cAMP functions extracellularly as the chemoattractant during aggregation and intracellularly to activate protein kinase A (PKA) (3). Upon starvation, *Dictyostelium* cells enter a development program that includes cAMP production, activation of PKA, and signal relay in which cAMP is secreted from cells (3, 35, 59). To determine if the internal cAMP relay system is involved in SMEK's translocation, we assayed HA-SMEK localization in *acaA*⁻/*acrA*⁻ and *PKA-R*⁻ backgrounds. *acaA*⁻/*acrA*⁻ cells lack the two adenylyl cyclases expressed during *Dictyostelium* growth and development, ad-

FIG. 1. Discovery and primary structure of SMEK (suppressor of *mek1*⁻). (A) Developmental morphology of KAx-3 (wild-type), *mek1*⁻, and *mek1*⁻/*smkA*⁻ strains at the mound stage of development. (B) Comparison of full-length *Dictyostelium* (Dd) and human (Hs) (DictyBase gene DDB0188242 and GenBank gene ID 55671) SMEK domain structures. A/B indicates a conserved acidic/basic stretch. (C) Amino acid sequence alignment of SMEK homologs *Dictyostelium discoideum* SMEK (www.dictybase.org, DDB0188242), *Homo sapiens* SMEK-1 (GenBank gene ID 55671) (which is expressed as a full-length variant 1 and a C-terminally truncated variant 2), *H. sapiens* SMEK-2 (GenBank gene ID 57223), *Xenopus laevis* (Xl) SMEK (GenBank accession number XM 048092), *Drosophila melanogaster* (Dm) SMEK (GenBank gene ID 41675 and www.flybase.bio.indiana.edu *falafel*), and *S. cerevisiae* SMEK (GenBank gene ID 213192). The red box shows the N-terminal EVH1 domain, the blue box shows the DUF-625 domain, and the black box shows the C-terminal conserved acidic/basic stretch. Asterisks indicate the conserved Y and W found in other type I EVH1 domains. Residues identical between the homologs are highlighted in yellow, incompletely conserved residues are in blue, and similar residues are in light green.

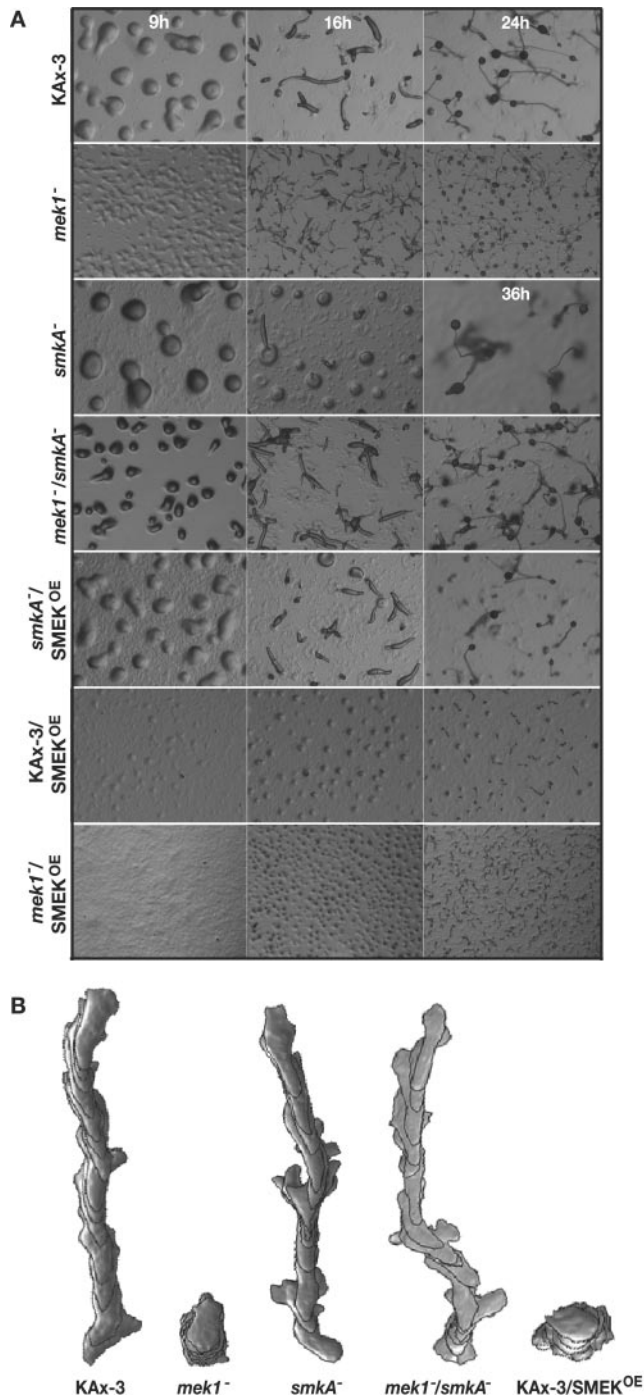


FIG. 2. *smkA*⁻ and Ax3/SMEK^{OE} development and chemotaxis profiles. (A) Developmental morphology of KAx-3, *mek1*⁻, *smkA*⁻, *mek1*⁻/*smkA*⁻, *smkA*⁻/SMEK^{OE}, KAx-3/SMEK^{OE}, and *mek1*⁻/SMEK^{OE} strains. Development at 9 h (wild-type mound stage), 16 h (wild-type slug stage), and 24 h (wild-type stalk and fruiting body stage) is shown. A 36-h time point is shown for the *smkA*⁻ strain, rather than 24 h, because the *smkA*⁻ cells do not form fruiting bodies until that time. (B) Representative traces of wild-type KAx-3, *mek1*⁻, *smek*⁻, *mek1*⁻/*smek*⁻, and SMEK^{OE} strains moving up a gradient towards a pipette filled with 150 μ M cAMP. Time-lapse recordings were taken at 6-s intervals; superimposed images show the cell shape, direction, and length of path at 1-min intervals.

enylyl cyclases A (ACA) and R (ACR). Thus, the double knockout strain should not produce cAMP and does not aggregate (2, 51). HA-SMEK localizes to the cell cortex in vegetative *acaA*⁻/*acrA*⁻ cells and translocates to the nucleus within 1 h of starvation (data not shown). *PKA-R*⁻ cells lack the regulatory subunit of PKA and aggregate precociously due to a constitutively active PKA (49). In the *PKA-R*⁻ background, HA-SMEK also localizes to the cell cortex in the vegetative state and to the nucleus on starvation (data not shown). Thus, SMEK's translocation is regulated by a starvation signal other than the established cAMP-PKA pathway.

Many proteins containing EVH1 domains localize to F-actin-rich regions via polyproline substrate-EVH1 domain interactions (43). To determine if SMEK's EVH1 domain is required for the cortical localization of SMEK in vegetative cells, we examined the subcellular distribution of an HA-SMEK construct missing the N-terminal 110 residues (Fig. 5A, SMEK ^{Δ EVH1}) and of an HA-SMEK construct containing only the EVH1 domain (Fig. 5A, EVH1). In KAx-3 cells, SMEK ^{Δ EVH1} constitutively localizes to the nucleus, even during vegetative growth (Fig. 5B). In contrast, the EVH1 domain constitutively localizes to the cell cortex, even after starvation (Fig. 5C). We observed identical localization patterns in *smkA*⁻ and *mek1*⁻/*smkA*⁻ backgrounds (data not shown). Therefore, SMEK's EVH1 domain is necessary and sufficient for its cortical localization.

To determine which SMEK residues are responsible for its nuclear localization, we analyzed the localization of HA-tagged SMEK¹⁻⁸¹¹, which is truncated at residue 811 after the conserved EVH1 and DUF625 domains. SMEK¹⁻⁸¹¹ is distributed throughout the cytoplasm and at the cell cortex in both vegetative cells and cells pulsed with cAMP (data not shown). We searched SMEK's C terminus for a canonical NLS, which is typically a short sequence of positively charged residues. Although most of the sequence after residue 811 is unconserved simple sequence, the C terminus contains a short, conserved stretch of acidic residues, followed by basic residues (Fig. 1B and C; residues 1006 to 1026). We created an HA-tagged SMEK deletion construct that lacked the conserved C-terminal basic stretch (Fig. 5A, SMEK ^{Δ NLS}, residues 1 to 1018) and the terminal residues. We also created a second, control construct that retained the positively charged domain but lacked the C-terminal residues (Fig. 5A, SMEK ^{Δ C}, residues 1 to 1026). Both constructs localize to the cell cortex and cytoplasm in vegetatively growing KAx-3 cells, similar to full-length SMEK (Fig. 5D and E). After cAMP pulsing, SMEK ^{Δ NLS} remains at the cell cortex, while SMEK ^{Δ C} translocates to the nucleus. Thus, the conserved basic residues near the C terminus serve as an NLS to target SMEK to the nucleus in response to a starvation signal.

SMEK^{OE} phenotypes are dependent on SMEK's subcellular localization. We employed these differentially localizing mutants and the different wild-type, SMEK^{OE}, and *smkA*⁻ phenotypes to determine whether SMEK functions at the cell cortex and/or in the nucleus during chemotaxis. In addition to assaying chemotaxis parameters, we focused on two developmental phenotypes: aggregation efficiency (which is reduced by SMEK overexpression) and mound size (which is reduced by loss of MEK1 and suppressed by simultaneous loss of SMEK). In contrast to expression of full-length SMEK, expression of

TABLE 1. Phenotypes of strains expressing differentially localizing SMEK mutants

Strain	HA-SMEK ^a	Localization ^b		Phenotype			
		Veg	Starve	Agg ^c	Mound size ^d	Cell polarity ^e	Chemotaxis ^f
KAx-3	NA	NA	NA	+++	+++	+++	+++
<i>mek1</i> ⁻	NA	NA	NA	+++	+	+	+
<i>smkA</i> ⁻	NA	NA	NA	+++	+++	+++	+++
<i>mek1</i> ⁻ / <i>smkA</i> ⁻	NA	NA	NA	+++	++	+++	+++
<i>smkA</i> ⁻	SMEK ^{OE}	C	N	+++	+++	++	++
KAx-3	SMEK ^{OE}	C	N	+	+++	+	+
KAx-3	SMEK ^{ΔEVH1}	N	N	+++	+++	+++	+++
KAx-3	SMEK ^{ΔNLS}	C	C	+	+++	+	+
KAx-3	SMEK ^{ΔC}	C	N	+	+++	+	+
<i>mek1</i> ⁻ / <i>smkA</i> ⁻	SMEK ^{OE}	C	N	+	+	+	+
<i>mek1</i> ⁻ / <i>smkA</i> ⁻	SMEK ^{ΔEVH1}	N	N	+++	+	+	+
<i>mek1</i> ⁻ / <i>smkA</i> ⁻	SMEK ^{ΔNLS}	C	C	+	++	+++	++
<i>mek1</i> ⁻ / <i>smkA</i> ⁻	SMEK ^{ΔC}	C	N	+	+	+	+

^a All HA-SMEK constructs are overexpressed. NA, not applicable.

^b Localization of SMEK constructs during vegetative growth (Veg) and after 6 h in Na-K phosphate buffer with cAMP pulses (Starve). N, nucleus; C, cell cortex.

^c Reflection of percentage of cells aggregating after 9 h of development. +, a lawn of unaggregated cells persists; +++, most cells aggregate and form developmental structures.

^d +, tiny *mek1* mounds; ++, medium-sized mounds; +++, wild-type-sized mounds.

^e Cell polarity reflects a lack of roundness. +++, 45 to 60% roundness; ++, 60 to 70% roundness; +, >70% roundness.

^f Chemotaxis speed and directionality, a measure of the linearity of the path. Cells moving in a straight line to the needle have a directionality of 1.0. +, 1 to 4 μm/min and 0 to 0.4 directionality; ++, 5 to 8 μm/min and 0.4 to 0.6 directionality; +++, 8 to 10 μm/min and 0.6 to 0.9 directionality.

SMEK^{ΔEVH1} in wild-type cells does not reduce the efficiency of aggregation (Fig. 6A; Table 1) and only mildly reduces cell polarization and directionality during chemotaxis up a cAMP gradient (Fig. 6B; Tables 1 and 2). The lack of overexpression phenotypes with a construct that constitutively localizes to the nucleus suggests that the overexpression phenotype is due to SMEK activity at the cell cortex. This hypothesis was corroborated by analysis of the C-terminal deletion mutants. Expression of SMEK^{ΔNLS} and SMEK^{ΔC} in wild-type KAx-3 cells reduces the cells' ability to join the developing mounds. These strains exhibit slower aggregation and delayed progression through the multicellular stages, similar to, but not as severe as, what is seen in KAx-3 cells overexpressing full-length SMEK (Fig. 6A). When put in a cAMP gradient, KAx-3/SMEK^{ΔNLS} and KAx-3/SMEK^{ΔC} cells chemotax poorly, with a

speed of 5 μm/min, 0.35 and 0.43 directionality, and 58 and 64% roundness, respectively. These parameters resemble, but are not as severe as, the chemotaxis defects of KAx-3 cells overexpressing full-length SMEK (Fig. 6B; Tables 1 and 2). Thus, high levels of SMEK at the cell cortex are sufficient to reduce cell polarity and chemotaxis speed and directionality. As the phenotypes of KAx-3/SMEK^{ΔC} cells are not as strong as those of KAx-3/SMEK cells, we suggest that the C-terminal residues of SMEK contribute to the overexpression phenotype seen in KAx-3/SMEK^{OE} cells.

Because these overexpression phenotypes complicated the phenotypic read-outs when we examined the ability of SMEK^{ΔEVH1}, SMEK^{ΔNLS}, and SMEK^{ΔC} to complement the *smkA* deficiency, we assayed for complementation of *smkA* deficiency in the *mek1*⁻/*smkA*⁻ background. In the wild-type background, *smkA*⁻ cells aggregate normally but exhibit a delayed exit from the mound stage. In the *mek1*⁻ background, *smkA* deficiency causes a stark increase in mound size during development (*mek1*⁻/*smkA*⁻ cells compared to *mek1*⁻ cells) and improves cell polarity and chemotaxis speed and directionality to the levels of wild-type cells. Thus, SMEK is required for the *mek1*⁻ aggregation and chemotaxis defects. Expression of full-length SMEK in *mek1*⁻/*smkA*⁻ cells should revert the strain to the *mek1*⁻ phenotype and lead to the formation of tiny aggregates and reduced chemotaxis. This is what is observed (Fig. 6A and B). *mek1*⁻/*smkA*⁻/SMEK^{OE} cells form aggregates with tiny mounds during development and chemotax with a speed of 3.4 μm/min, 0.2 directionality, and 77% roundness, similar to *mek1*⁻ cells. Many of the cells do not enter the mounds, which we attribute to the SMEK^{OE} phenotype.

We examined the ability of either cytoplasmic- or nuclear-localized SMEK to complement SMEK deficiency by expressing the SMEK deletion mutants (which are constitutively found in either the cytoplasm or the nucleus) in *mek1*⁻/*smkA*⁻ cells. If SMEK must localize to the nucleus to cause the *mek1*⁻

TABLE 2. DIAS program analysis of chemotaxis

Strain	Speed (μm/min) ^{a,b}	Directionality ^{a,c}	Roundness (%) ^{a,d}
KAx-3	10.97 ± 1.07	0.82 ± 0.03	46.54 ± 1.67
<i>mek1</i> ⁻	3.35 ± 0.43	0.14 ± 0.04	72.59 ± 4.05
<i>smkA</i> ⁻	8.62 ± 0.35	0.76 ± 0.05	46.53 ± 1.84
<i>mek1</i> ⁻ / <i>smkA</i> ⁻	9.98 ± 1.29	0.67 ± 0.04	47.88 ± 2.14
KAx-3/SMEK ^{OE}	3.31 ± 0.37	0.17 ± 0.05	76.38 ± 1.67
KAx-3/SMEK ^{ΔEVH1}	10.18 ± 1.18	0.69 ± 0.02	51.24 ± 1.99
KAx-3/SMEK ^{ΔNLS}	4.71 ± 0.74	0.35 ± 0.06	58.21 ± 3.61
KAx-3/SMEK ^{ΔC}	4.54 ± 0.72	0.43 ± 0.09	64.06 ± 4.98
<i>mek1</i> ⁻ / <i>smkA</i> ⁻ /SMEK ^{OE}	3.39 ± 0.40	0.22 ± 0.06	77.09 ± 4.57
<i>mek1</i> ⁻ / <i>smkA</i> ⁻ /SMEK ^{ΔEVH1}	2.51 ± 0.25	0.16 ± 0.01	83.87 ± 2.79
<i>mek1</i> ⁻ / <i>smkA</i> ⁻ /SMEK ^{ΔNLS}	5.42 ± 0.09	0.42 ± 0.04	56.93 ± 1.77
<i>mek1</i> ⁻ / <i>smkA</i> ⁻ /SMEK ^{ΔC}	2.26 ± 0.20	0.07 ± 0.04	89.66 ± 2.19

^a Values are means ± standard errors of the means for at least five cells (110 frames/cell).

^b Speed of cell's centroid movement along the total path.

^c Directionality is a measurement of the linearity of the path. Cells moving in a straight line to the needle have a directionality of 1.00.

^d Roundness is a measurement of the lack of cell polarity. A high percent roundness indicates that the cells are more round and less polarized.

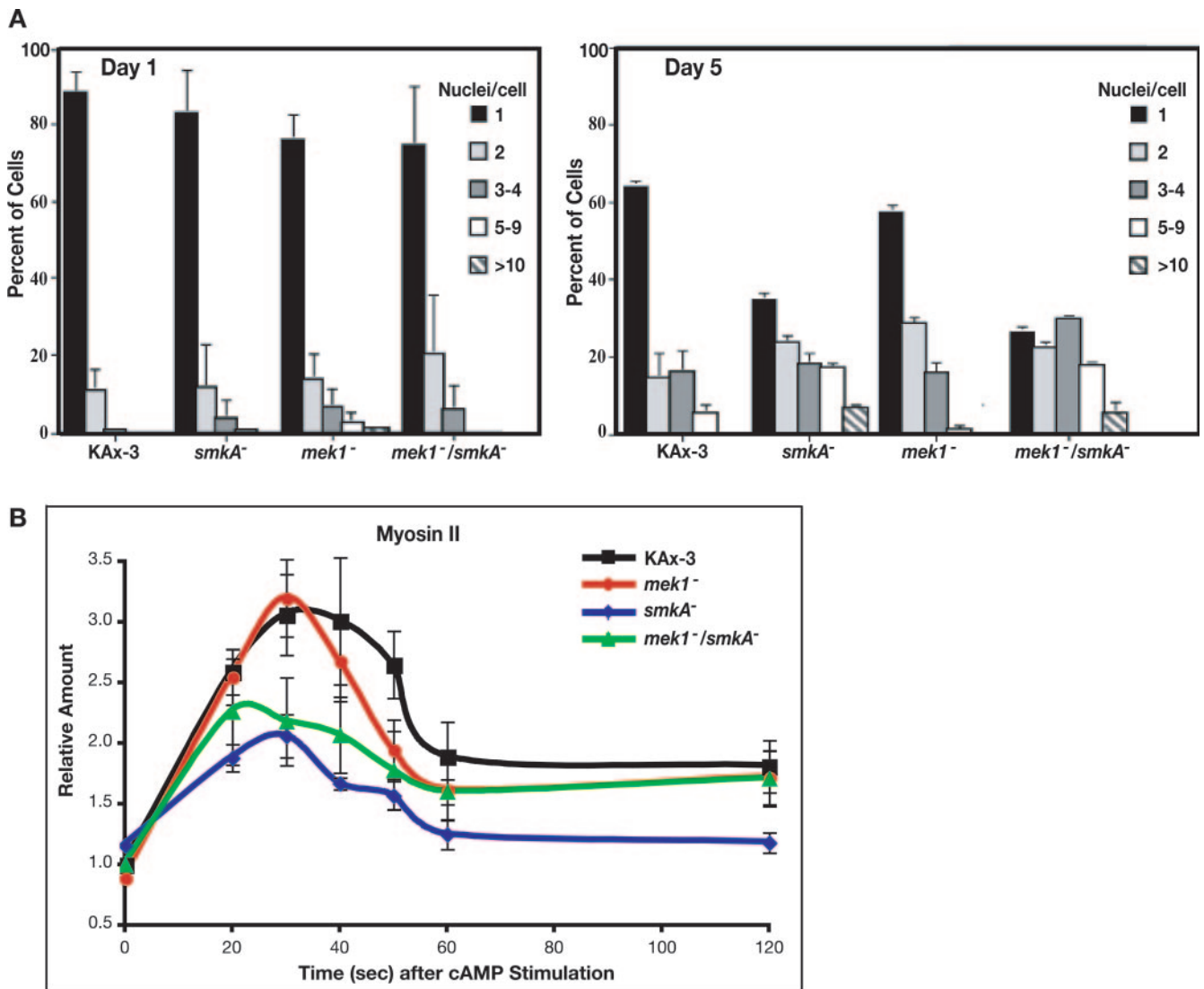


FIG. 3. *smkA*⁻ and *mek1*⁻/*smkA*⁻ cells exhibit defects in cytokinesis and myosin II assembly. (A) Quantitation of the percentage of cells with 1, 2, 3 or 4, 5 to 9, and 10 or more nuclei after growth in shaking culture for 1 and 5 days for KAx-3, *smkA*⁻, *mek1*⁻, and *mek1*⁻/*smkA*⁻ strains. Error bars represent standard errors of the means for multiple experiments. (B) Kinetics of myosin II accumulation in the Triton X-100-insoluble fraction in response to cAMP stimulation. All values depicted are relative to the amount of myosin II at time zero for the wild-type KAx-3 reference cells. Error bars represent standard errors from multiple experiments.

chemotaxis defects, then expression of SMEK^{ΔEVH1} and SMEK^{ΔC} in *mek1*⁻/*smkA*⁻ cells should complement the *smkA* deletion, similar to expression of full-length SMEK. Thus, SMEK^{ΔEVH1} and SMEK^{ΔC} should restore the *mek1*⁻ phenotype when expressed in *mek1*⁻/*smkA*⁻ cells; i.e., the *mek1*⁻/*smkA*⁻/SMEK^{ΔEVH1} and *mek1*⁻/*smkA*⁻/SMEK^{ΔC} strains should form tiny mounds and have severe chemotaxis defects resembling those of *mek1*⁻ cells and *mek1*⁻/*smkA*⁻/SMEK^{OE} cells. In contrast, expression of the cytoplasmically localized SMEK^{ΔNLS} in *mek1*⁻/*smkA*⁻ cells would not be expected to complement SMEK deficiency during chemotaxis, and the strain's mound size and chemotaxis parameters should resemble those of *mek1*⁻/*smkA*⁻ cells.

Interestingly, expression of SMEK^{ΔEVH1} reverts the double knockout strain to the *mek1*⁻ tiny-mound and inhibited-che-

motaxis phenotypes, similar to expression of full-length SMEK (Fig. 6B; Tables 1 and 2). *mek1*⁻/*smkA*⁻/SMEK^{ΔEVH1} cells form tiny mounds during development and chemotax with a speed of 3 μm/min, 0.16 directionality, and 84% roundness. SMEK^{ΔEVH1} complementation of *smkA* deficiency in the *mek1*⁻/*smkA*⁻ background suggests that SMEK functions in the nucleus to cause the *mek1*⁻ phenotype.

We confirmed this hypothesis with the cytoplasmically localizing SMEK^{ΔNLS} mutant. As with *mek1*⁻/*smkA*⁻/SMEK^{OE} cells, many *mek1*⁻/*smkA*⁻/SMEK^{ΔNLS} and *mek1*⁻/*smkA*⁻/SMEK^{ΔC} cells do not join the developing aggregates, which we attribute to the overexpression of SMEK. However, the *mek1*⁻/*smkA*⁻/SMEK^{ΔNLS} mounds, slugs, and fruiting bodies that form are the sizes of *mek1*⁻/*smkA*⁻ structures, not those of *mek1*⁻ cells. These data indicate that during aggregation,

KAX-3/HA-SMEK

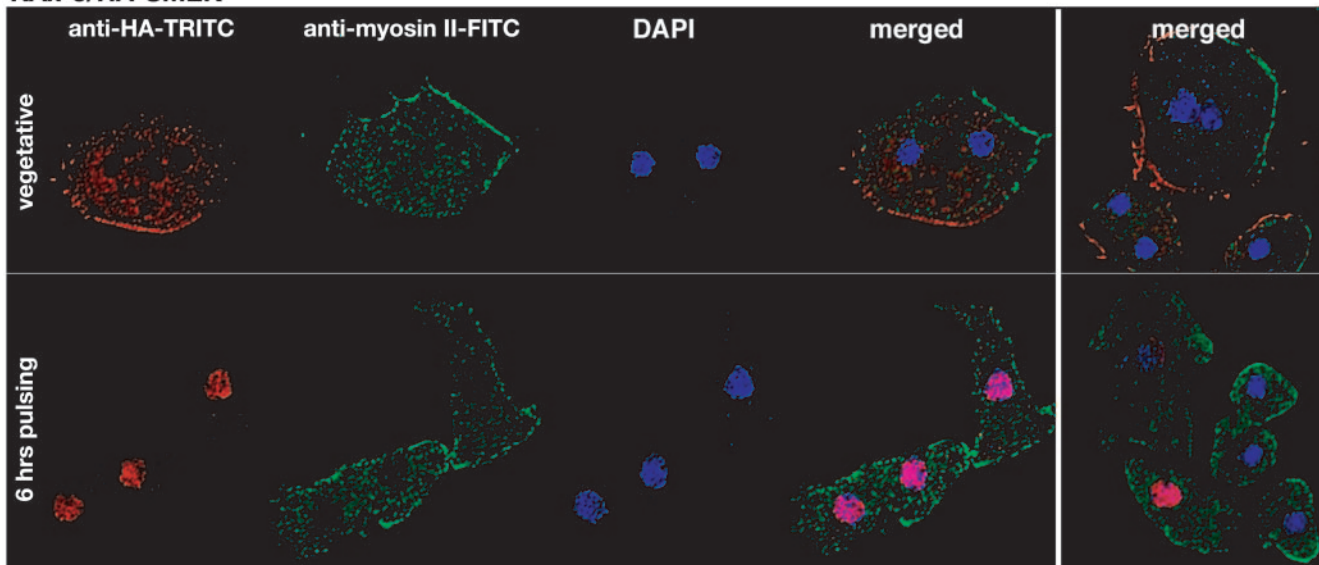


FIG. 4. SMEK localizes to the cell cortex in vegetative cells and translocates to the nucleus during starvation. Localization of full-length HA-SMEK and myosin II in vegetative and chemotaxing (cAMP-pulsed) KAX-3 cells is shown. Cells were labeled with DAPI (4',6'-diamidino-2-phenylindole) stain (blue) to demarcate the nuclei and with HA (red) and myosin II (green) antibodies. Each image represents a deconvolved integration of multiple optical sections through the given cell sample. TRITC, tetramethyl rhodamine isocyanate; FITC, fluorescein isothiocyanate.

the absence of SMEK cannot be complemented by the cytoplasmically localizing SMEK^{ΔNLS} mutant (Fig. 2A and 6A; Table 1). The *mek1*⁻/*smkA*⁻/SMEK^{ΔNLS} strain also exhibits a partially suppressed *mek1*⁻ chemotaxis phenotype (Table 2) (speed of 5.4 μm/min, 0.4 directionality, and 57% roundness). Thus, the NLS is required for full SMEK function and complementation of the *smkA*⁻ defects in the *mek1*⁻ background (Fig. 6B). The control *mek1*⁻/*smkA*⁻/SMEK^{ΔC} strain, like *mek1*⁻/*smkA*⁻/SMEK^{OE} cells, forms tiny mounds, slugs, and fruiting bodies that resemble *mek1*⁻ structures (Fig. 2A and 6A). *mek1*⁻/*smkA*⁻/SMEK^{ΔC} cells chemotax with a speed of 2 μm/min, 0.07 directionality, and 90% roundness, similar to *mek1*⁻ cells (Table 2). This indicates that expression of SMEK^{ΔC} can complement the *smkA*⁻ deficiency in *mek1*⁻/*smkA*⁻ cells and revert the cells to a *mek1*⁻ phenotype, similar to expression of full-length SMEK and SMEK^{ΔEVH1}. These differences in the phenotypes of *mek1*⁻/*smkA*⁻ cells expressing either SMEK^{ΔEVH1}, SMEK^{ΔNLS}, or SMEK^{ΔC} are consistent with a model in which SMEK must localize to the nucleus to cause the *mek1*⁻ chemotaxis defects. We expect that the partially suppressed *mek1*⁻ chemotaxis phenotype of *mek1*⁻/*smkA*⁻/SMEK^{ΔNLS} cells may be due to the cytoplasmically localized overexpression phenotype. Another possibility would be that some of the SMEK^{ΔNLS} protein is nuclearly localized.

***smek*⁻ suppresses *mek1*⁻ defects in gene expression.** The immunofluorescence and phenotype analyses indicate that SMEK translocates to the nucleus upon starvation and that this translocation is required for the *mek1*⁻ chemotaxis defects. From these data and studies with many systems demonstrating that MAP kinase pathways can control the transcription of specific genes, we hypothesized that the MEK1/ERK1 pathway regulates gene expression during chemotaxis and that SMEK is partly responsible for any erroneous gene expression

in *mek1*⁻ cells (21). Because the MEK1/ERK1 pathway gene targets in *Dictyostelium* have not been characterized, we indirectly assayed the transcription of 600 developmental genes in KAX-3, *mek1*⁻, *erk1*⁻, *smkA*⁻, and *mek1*⁻/*smkA*⁻ strains with microarrays. These 600 genes were chosen from the set of 6,345 probes previously analyzed on microarrays (24): ~250 genes exhibited a ≥3-fold increase in expression during development, ~250 genes exhibited a ≥3-fold decrease, and ~100 genes were chosen because of developmental interest and are listed at <http://www.biology.ucsd.edu/loomis-cgi/microarray/Smek-array.html>. We developed the strains in shaking culture with cAMP pulsing and harvested their RNAs every 2 h (24, 37, 48). The RNA was fluorescently labeled and compared to labeled, time-averaged reference RNA. Two independent experiments showed good reproducibility; the average values for individual genes can be found at <http://www.biology.ucsd.edu/loomis-cgi/microarray/Smek-array.html>.

Dramatic changes in gene expression coincide with *Dictyostelium*'s transition from a unicellular into a multicellular organism (24, 37, 57). One such transition occurs after 10 h of development, when the unicellular aggregating cells form loose multicellular mounds (3, 26). We discovered that *mek1*⁻ and *erk1*⁻ cells precociously express a number of the late genes involved in this transition (after only 4 to 8 h of development) (Fig. 7). This phenomenon was not observed in *smkA*⁻ cells and was partially suppressed in *mek1*⁻/*smkA*⁻ cells (16 out of 19 precocious genes were suppressed). Two of the genes expressed precociously in *mek1*⁻ and *erk1*⁻ cells (DDB0231389 and DDB0231081) were completely dependent on the presence of SMEK. The other 14 gene transcripts that showed increases in *mek1*⁻ and *erk1*⁻ cells (compared with wild-type cells) were only partly dependent on SMEK. SMEK deficiency in *mek1*⁻ cells reduced the induction level of these latter genes

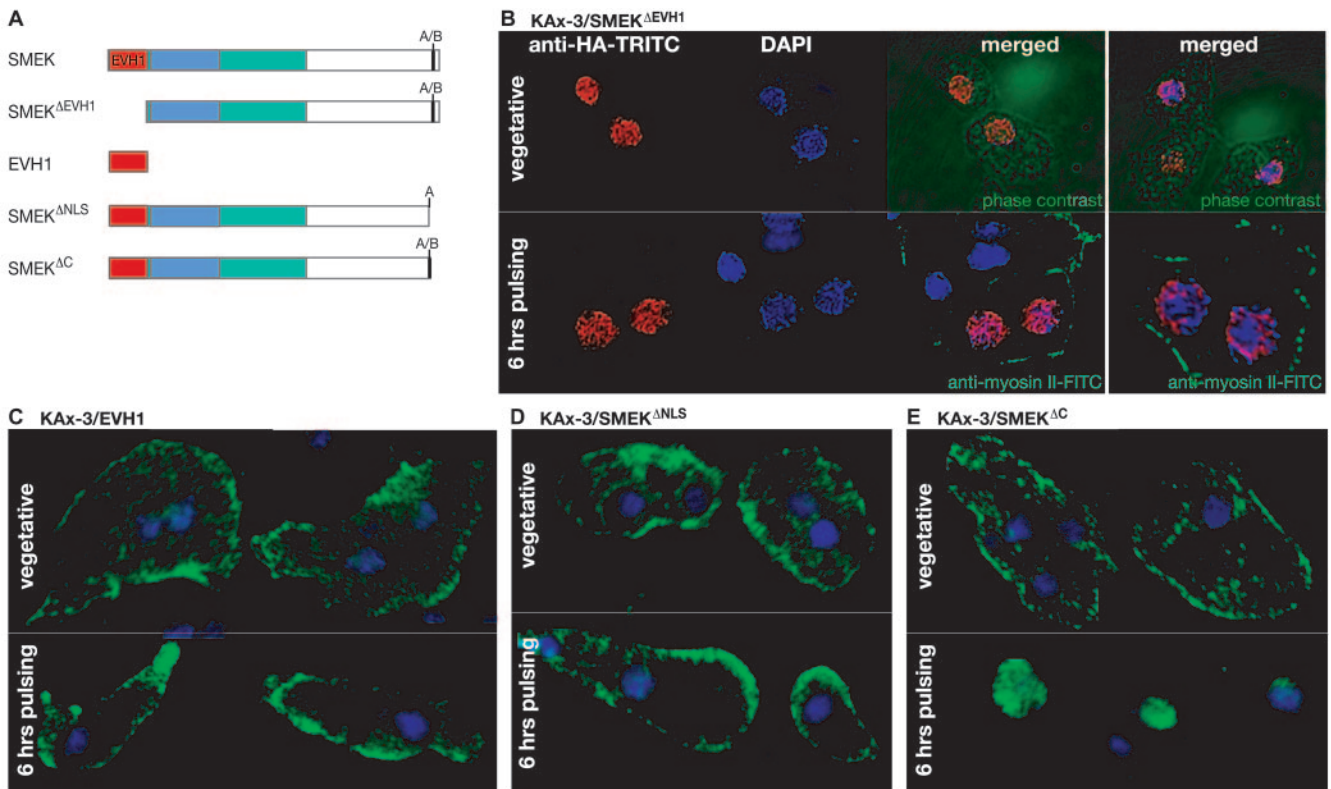


FIG. 5. SMEK localization is regulated by its EVH1 domain and an NLS at the C terminus. (A) SMEK deletion constructs. All constructs are HA tagged. (B) Confocal images show the localization of SMEK Δ EVH1 (red) in vegetative KAx-3 cells and cells pulsed with cAMP for 6 h. The merged vegetative cell image is superimposed on a phase-contrast image; the merged pulsed-cell image is superimposed on a myosin II-stained image (green) to demarcate the cell bodies. TRITC, tetramethyl rhodamine isocyanate; FITC, fluorescein isothiocyanate. DAPI, 4',6'-diamidino-2-phenylindole. (C to E) Confocal images show KAx-3 cells expressing EVH1 (C), SMEK Δ NLS (D), and SMEK Δ C (E).

from ≥ 10 - to 20-fold to less than 6-fold in most cases. We confirmed the precocious expression of *tagB* and *tipB* mRNA in *mek1* $^{-}$ cells and its suppression in *mek1* $^{-}/smkA$ $^{-}$ cells by Northern blotting of RNA prepared in a third independent experiment (Fig. 7B).

This pattern of precocious late gene expression in *mek1* $^{-}$ and *erk1* $^{-}$ cells parallels their precocious transition from mounds to slugs (Fig. 2A and data not shown). The suppression of precocious gene expression in *mek1* $^{-}/smkA$ $^{-}$ cells also resembles the suppression of the *mek1* $^{-}$ developmental defects (Fig. 2A), in which the *mek1* $^{-}/smkA$ $^{-}$ time of transition to later developmental stages resembles that of wild-type cells.

smkA $^{-}$ cells did not exhibit any major differences in the global gene expression patterns compared to wild-type cells. However, one gene, *pdiA*, an inhibitor of cAMP phosphodiesterase normally expressed at 4 h of development, is not expressed in *smkA* $^{-}$ or in *mek1* $^{-}/smkA$ $^{-}$ cells (Fig. 7A and B). These results make it unlikely that SMEK is a global regulator of gene expression. Instead, SMEK contributes to the high levels of precocious late gene expression seen in *mek1* $^{-}$ cells and is required for the expression of a second set of MEK1-independent genes, represented by *pdiA*. PDIA is a secreted protein that binds to and inhibits the extracellular phosphodiesterase that degrades the extracellular cAMP chemoattractant and morphogen. PDIA expression is regulated by the levels of cAMP and is normally induced early in development

(16). While overexpression of PDI leads to developmental defects, the loss of PDI does not lead to visible developmental phenotypes (63), and thus the absence of PDI expression in *smkA* $^{-}$ cells would, in itself, not account for *smkA* $^{-}$ cell phenotypes.

DISCUSSION

Dictyostelium and mammalian cells must activate the MEK/ERK pathway in order to chemotax effectively (20, 34, 36, 39, 65). However, questions remain about where the MEK/ERK kinases function during chemotaxis and which molecules are responsible for the defective chemotaxis in their absence. We have discovered and characterized an evolutionarily conserved protein that is required for the *Dictyostelium* *mek1* $^{-}$ cell polarity and chemotaxis defects. SMEK is the founding member of a highly conserved protein family found in the genomes of all eukaryotes examined, including yeast, *Dictyostelium*, *Arabidopsis*, *Drosophila*, *Xenopus*, and humans (Fig. 1C).

SMEK's highly conserved functional domains. The two most highly conserved regions of SMEK are the N-terminal EVH1 domain and the central domain, which suggests these are the critical functional domains. The EVH1 domains of ENA/VASP and Homer target the signaling proteins to actin-rich focal adhesions and neuronal synaptic signaling domains, respectively (5, 22, 30). We found that SMEK's EVH1 domain

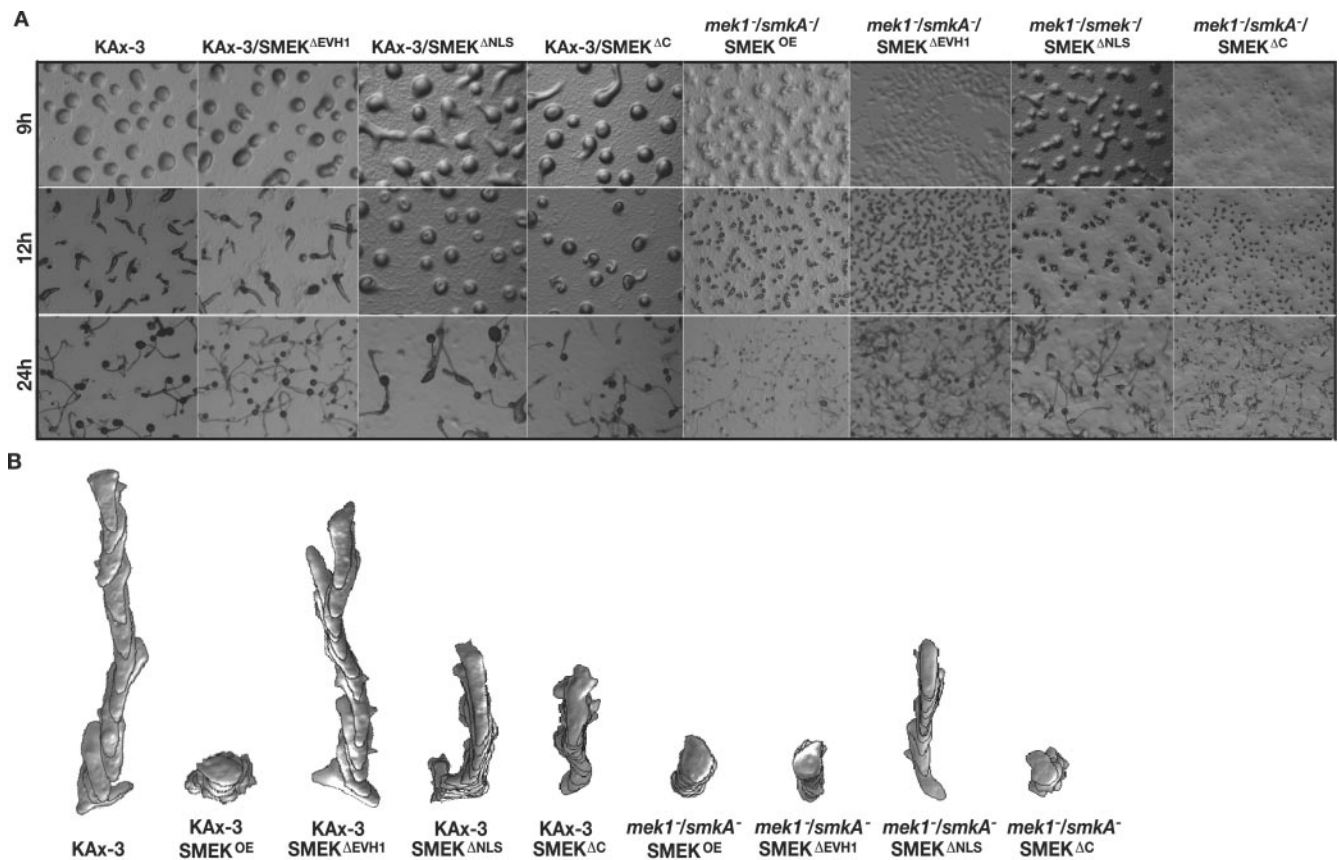


FIG. 6. SMEK^{ΔEVH1}, SMEK^{ΔNLS}, and SMEK^{ΔC} development and chemotaxis profiles. (A) Developmental morphology of KAx-3 and *mek1-/smkA-* strains expressing SMEK, SMEK^{ΔEVH1}, SMEK^{ΔNLS}, and SMEK^{ΔC}. (B) Representative traces of strains moving up a gradient towards a pipette filled with 150 μ M cAMP. Time-lapse recordings were taken at 6-s intervals; superimposed images show the cell shape, direction, and length of path at 1-min intervals. The KAx-3/SMEK^{OE} trace is taken from Fig. 2B.

is required for its localization to the cell cortex. SMEK^{ΔEVH1}, which lacks the EVH1 domain, constitutively localizes to the nucleus, and the isolated EVH1 domain constitutively localizes to the cell cortex. SMEK's central domain consists of an uncharacterized conserved domain (PFAM DUF625). Because expression of SMEK^{ΔEVH1} complements loss of SMEK in *mek1-/smkA-* cells and the C terminus is not well conserved, we suggest that this central domain mediates SMEK's function. The characterization of this novel, conserved domain and its role in chemotaxis signaling should provide insights into the molecular mechanism of SMEK function.

Careful alignment of the SMEK homologs revealed a third partially conserved domain at the very C terminus of the SMEK protein. This domain consists of a stretch of acidic residues followed by basic residues and is found in SMEK proteins from higher eukaryotes and *Dictyostelium* but not *Saccharomyces cerevisiae*. We show that the basic stretch is required for *Dictyostelium* SMEK's translocation to the nucleus in response to starvation. We propose that this domain is an NLS that is exposed by a starvation-induced change in the conformation of the SMEK C terminus.

Loss of SMEK results in reduced myosin II assembly in response to chemoattractant stimulation. In addition to partially suppressing *mek1-* chemotaxis defects, SMEK deficiency

causes reduced cytokinesis during growth in shaking culture and delayed exit from the mound stage during morphogenesis. These phenotypes are similar to, but less severe than, those of strains with mutations that block myosin II assembly (9, 11, 18). Thus, the reduced cytokinesis and retarded morphogenesis are consistent with *smkA-* cells having reduced myosin II assembly. We report that *smkA-* cells exhibit reduced myosin II accumulation at the cell cortex, compared to wild-type cells, in response to chemoattractant stimulation. However, mutations that lead to a reduced myosin II assembly rather than a complete (or almost complete) loss of myosin II assembly and their resultant phenotypes have not been characterized. This makes it difficult to definitely attribute the cytokinesis and mound delay phenotypes to reduced myosin II assembly.

SMEK translocation to the nucleus and functional implications. SMEK is found at the cortex in vegetatively growing cells but is nuclear in developing cells. Many chemotaxis signaling proteins (phosphatidylinositol 3-kinase, MEK1, ERK1, and PH domain-containing proteins [CRAC, PKB, and PhdA]) undergo a shift in subcellular localization to the cell cortex after chemoattractant stimulation. Interestingly, HA-SMEK translocates to the nucleus in *acaA-/acrA-* cells starved for only 1 h. Because these cells lack the two adenylyl cyclases normally expressed during vegetative growth and chemotaxis,

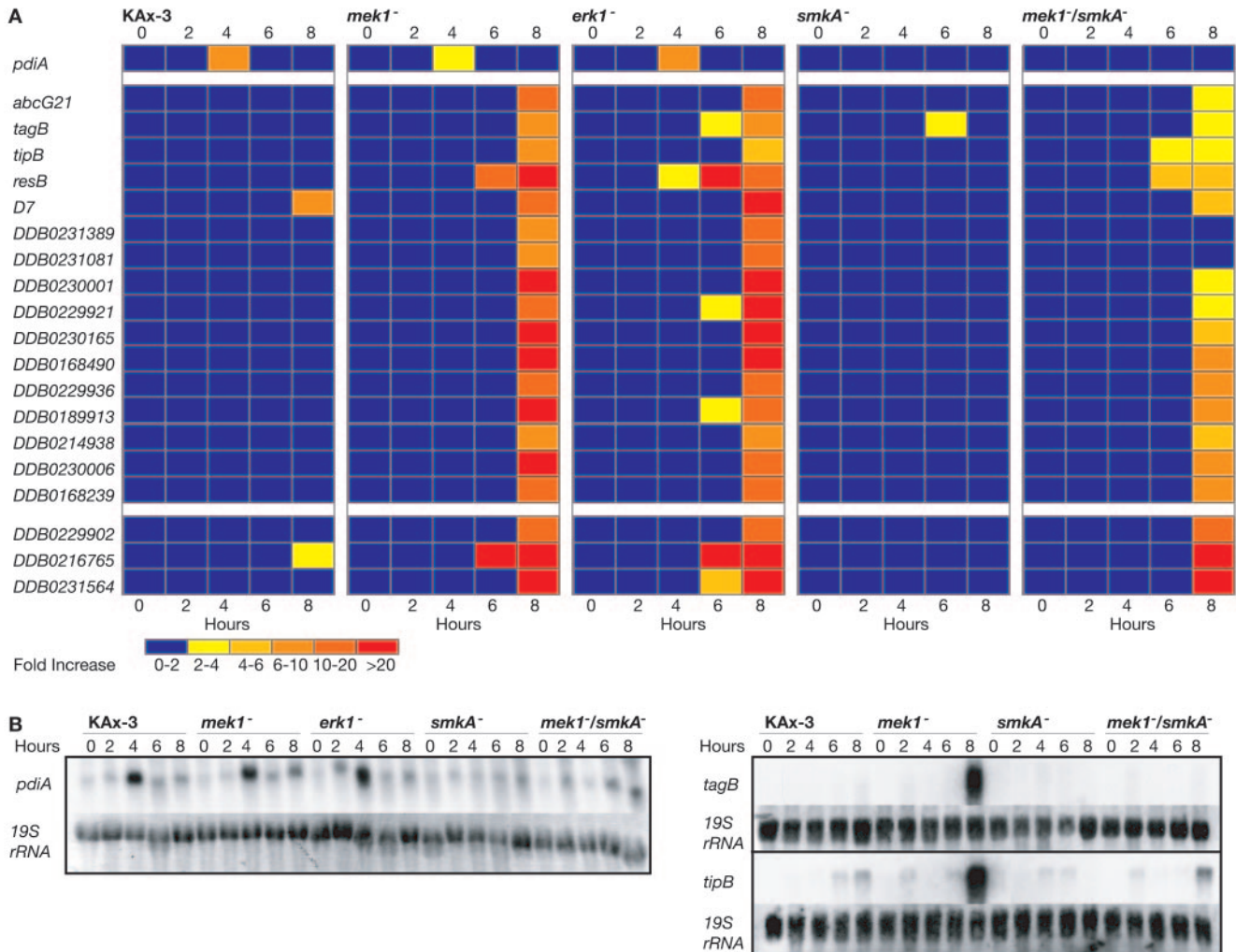


FIG. 7. Expression profiles of 20 genes during early development. (A) Bar graphs for the expression profile of each gene in KAx-3, *mek1*⁻, *erk1*⁻, *smkA*⁻, and *mek1*⁻/*smkA*⁻ cells represent the average change (*n*-fold). Absolute values for each target are at <http://www.biology.ucsd.edu/loomis/cgi/microarray/Smek-array.html>. The first gene listed, *pdiA*, is an early gene with SMEK-dependent expression after 4 h of development. The following genes are expressed precociously in *mek1*⁻ and *erk1*⁻ cells. Loss of SMEK reduces the level of precocious expression of 16 of the 19 genes but does not affect the remaining 3 out of 19 genes. (B) Northern analysis of *pdiA*, *tagB*, and *tipB* transcripts during development of KAx-3, *mek1*⁻, *erk1*⁻, *smkA*⁻, and *mek1*⁻/*smkA*⁻ cells.

the signal for translocation is unlikely to be chemoattractant stimulation or intracellular cAMP signaling. Furthermore, SMEK still localizes to the cell cortex in *PKA-R*⁻ cells, which have a constitutively active PKA. We propose that SMEK translocates in response to a cell density or starvation signal. Possible cAMP-independent starvation signals include the secreted prestarvation factor and conditioned medium factor. These factors are secreted in a cAMP-independent manner when growing *Dictyostelium* cells reach a high-density and low-nutrient state and are required for aggregation (10, 64).

By expressing the differentially localizing SMEK^{ΔEVH1} and SMEK^{ΔNLS} mutants in *mek1*⁻/*smkA*⁻ cells, we show that SMEK must be in the nucleus to mediate the *mek1*⁻ development and chemotaxis defects. We focused on the role of nuclear SMEK and found that SMEK is required for *mek1*⁻ elevated and precocious expression of late genes. The suppressed genes include *abcG21* and *tagB*, which encode ABC

transporters that couple the hydrolysis of ATP with chemical export in eukaryotes. ABC substrates include sugars and amino acids, hydrophilic drugs and lipids, and large proteins (1, 56). *abcG21* has not been characterized but is predicted to encode a full transporter with two ABC domains and two transmembrane domains (1). *tagB* encodes a half transporter with an N-terminal serine protease domain, a central transmembrane domain, and a C-terminal ABC domain. TagB is required for specialization of prestalk *pstA* cells, a subpopulation that develops in late mounds and forms the tip and eventually the stalk of the fruiting body (47). Consequently, *tagB*⁻ cells do not exit from the mound stage.

A third gene whose misregulation in *mek1*⁻ cells requires the presence of SMEK is *tipB*, whose protein product has no identified domains and whose biochemical activity has not been characterized. *tipB*⁻ cells are defective in the sorting of initial cell types in the mound and form aggregates with mul-

multiple small tips that occasionally proceed to form small, misshapen fruiting bodies (52). Many *tipB*⁻ cells do not join the developing mounds. Thus, we have identified two genes known to be required for exit from the mound stage (*tagB* and *tipB*) as being precociously expressed in *mek1*⁻ and *erk1*⁻ cells and suppressed in *mek1*⁻/*smkA*⁻ cells. This suggests that the MEK1/ERK1 pathway and SMEK oppositely regulate the expression of genes involved in exit from the mound stage to cause the early mound stage exit observed in *mek1*⁻ cells and the delayed exit observed in *smkA*⁻ cells.

The remaining genes identified as precociously expressed in *mek1*⁻ and *erk1*⁻ cells from the microarray have not been characterized yet. It is, however, known that expression of the *resB* transcript requires the MADS box transcription factor SrfA (14), possibly indicating another player in the signaling pathway. Our analysis also identified *pdiA* as being misregulated in *smkA*⁻ cells but not affected by MEK1 or ERK1.

At this time, it is unclear if these genes are candidates for explaining the *mek1*⁻, *erk1*⁻, *smkA*⁻, and *mek1*⁻/*smkA*⁻ phenotypes. Because the array covers only 5% of the *Dictyostelium* genome (600 of 12,000 predicted genes), future studies with the now completely sequenced genome may reveal genes more telling of the importance of MEK1/ERK1 transcriptional targets during chemotaxis. Because only a portion of the *mek1*⁻ and *erk1*⁻ misregulated genes are suppressed by *smkA* deletion, we favor a model in which SMEK acts independently of the MEK1/ERK1 pathway but inversely regulates the expression of some MEK1/ERK1 gene targets. Inherent in this model is the idea that MEK1/ERK1 regulation of gene expression is important for chemotaxis. For example, precocious late gene expression may interfere with the cells' ability to properly respond to signals for cell polarization and chemotaxis at earlier time points.

Our studies with SMEK deletion mutants also determined that expression of cell cortex-localized SMEK^{ΔNLS}, but not nuclearly localized SMEK^{ΔEVH1}, mimics the phenotypic effect of full-length SMEK overexpression. These data and the *smkA*⁻ cytokinesis defect during vegetative growth suggest that SMEK can function at the cell cortex in addition to in the nucleus (Fig. 8). Interestingly, cells expressing high levels of full-length SMEK protein, but not cells with high levels of SMEK^{ΔEVH1} protein, are selected against during growth (data not shown). This is consistent with the developmental and chemotaxis data, in which full-length SMEK, but not SMEK^{ΔEVH1}, causes phenotypic defects. Another possibility would be that, under conditions of overexpression, SMEK may localize differently from endogenous SMEK and excessive SMEK at the cell cortex may interact with binding partners not seen under endogenous expression levels. While studies with populations of these strains showed identical localization patterns in high- and low-expressing cells and the clones shown in Fig. 4 and 5 (M. Mendoza and R. Firtel, unpublished observations), knock-in experiments with *Dictyostelium* and studies with other organisms will be useful to determine whether SMEK's role in the nucleus during chemotaxis is conserved.

SMEK and the MEK1/ERK1 pathway: a genetic interaction. The discovery of SMEK as a suppressor of MEK1 leads to two possible modes of genetic interaction: (i) SMEK functions downstream of and is inhibited by MEK1, and (ii) SMEK acts independently of MEK1 but regulates some MEK1 effectors in

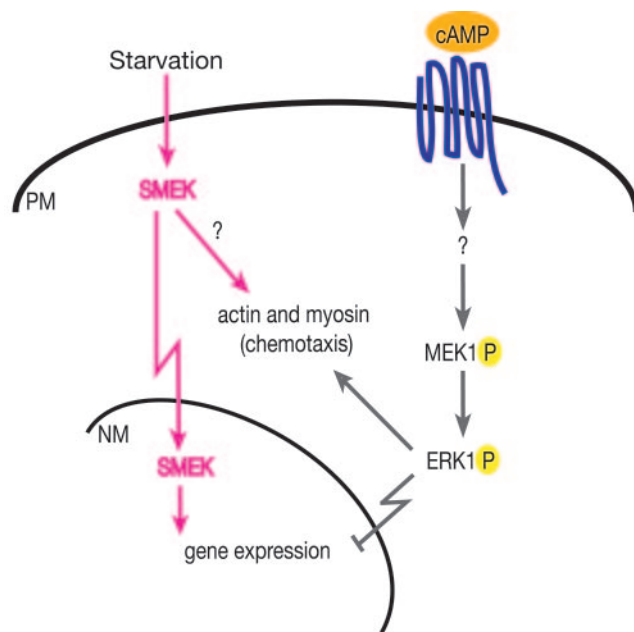


FIG. 8. Model of the regulation of *Dictyostelium* chemotaxis by MEK1 and SMEK. MEK1 and SMEK are in separate signaling pathways that converge on chemotaxis function through gene regulation in the nucleus or unknown cytoplasmic targets.

a manner opposite to that of the MEK1/ERK1 pathway (Fig. 8). The SMEK overexpression phenotype in *mek1*⁻ and *erk1*⁻ cells indicates that SMEK does not function solely downstream of the MEK1/ERK1 pathway. We have also found that expression of a constitutively active MEK1 in which the activation loop S/T phosphorylation sites are mutated to Glu (34) or of a hyperactive ERK1 with a mutation in the DE domain making it inefficiently dephosphorylated (45) in *smkA*⁻ cells causes delayed aggregation and defective chemotaxis phenotypes, similar to their expression in KAx-3 cells (Mendoza and Firtel, unpublished observation). Thus, MEK1/ERK1 signaling does not function solely through SMEK and may act both at the cortex and in the nucleus. We show that SMEK is only partially required for the *mek1*⁻ developmental phenotype and transcriptional defects, and loss of *smkA* causes MEK1/ERK1-independent phenotypes and transcriptional defects. Therefore, we favor the second model, in which the MEK1/ERK1 pathway and SMEK signaling converge on a partially overlapping set of effectors. This model includes the possibility that SMEK functions in a complex in which other members are regulated by the MEK1/ERK1 pathway and assumes the MEK1/ERK1 pathway has a broader range of downstream effectors than the ones requiring SMEK function.

In conclusion, we have characterized a novel, evolutionarily conserved protein required for *Dictyostelium* *mek1*⁻ defects during chemotaxis. SMEK responds to starvation by translocating to the nucleus. SMEK's nuclear localization is required for the *mek1*⁻ phenotype. Because SMEK has highly conserved homologs from yeast to humans, we suggest that SMEK regulation of *Dictyostelium* chemotaxis and the *mek1*⁻ and *erk1*⁻ phenotypes has parallels with SMEK function in mammalian systems. Further characterization of SMEK's binding

partners and biochemical activity in other systems will provide insight into both its own function and MEK1/ERK1 function in the nucleus during chemotaxis.

ACKNOWLEDGMENTS

We thank Tom Egelhoff for helpful suggestions and making available methods for chemoattractant-mediated cortical myosin II quantification. We thank James Ferimisco and the UCSD Cancer Center Imaging Facility for help with the deconvolution microscopy.

This work was supported by USPHS grants to W.F.L. and R.A.F.

ADDENDUM IN PROOF

While this paper was in press, a review on protein phosphatase 4 (P. T. W. Chohen, A. Philp, and C. Vázquez-Martin, *FEBS Lett.* **579**:3278–3286, 2005) listed the *S. cerevisiae* SMEK homolog sequence as a sequence identified in complex with protein phosphatase 4. The authors of this review propose that SMEK functions as a regulatory subunit of protein phosphatase 4.

REFERENCES

- Anjard, C., and W. F. Loomis. 2002. Evolutionary analyses of ABC transporters of *Dictyostelium discoideum*. *Eukaryot. Cell.* **1**:643–652.
- Anjard, C., F. Soderbom, and W. F. Loomis. 2001. Requirements for the adenyl cyclases in the development of *Dictyostelium*. *Development* **128**: 3649–3654.
- Aubry, L., and R. Firtel. 1999. Integration of signaling networks that regulate *Dictyostelium* differentiation. *Annu. Rev. Cell Dev. Biol.* **15**:469–517.
- Brahmbhatt, A. A., and R. L. Klemke. 2003. ERK and Rho differentially regulate pseudopodia growth and retraction during chemotaxis. *J. Biol. Chem.* **278**:13016–13026.
- Brakeman, P. R., A. A. Lanahan, R. O'Brien, K. Roche, C. A. Barnes, R. L. Haganir, and P. F. Worley. 1997. Homer: a protein that selectively binds metabotropic glutamate receptors. *Nature* **386**:284–288.
- Brown, M. C., and C. E. Turner. 2004. Paxillin: adapting to change. *Physiol. Rev.* **84**:1315–1339.
- Cheresh, D. A., J. Leng, and R. L. Klemke. 1999. Regulation of cell contraction and membrane ruffling by distinct signals in migratory cells. *J. Cell Biol.* **146**:1107–1116.
- Chisholm, R. L., and R. A. Firtel. 2003. Insights into morphogenesis from a simple developmental system. *Nat. Rev. Mol. Cell. Biol.* **5**:531–541.
- Chung, C., and R. A. Firtel. 1999. PAKa, a putative PAK family member, is required for cytokinesis and the regulation of the cytoskeleton in *Dictyostelium discoideum* cells during chemotaxis. *J. Cell Biol.* **147**:559–575.
- Clarke, M., and R. H. Gomer. 1995. PSF and CMF, autocrine factors that regulate gene expression during growth and early development of *Dictyostelium*. *Experientia* **51**:1124–1134.
- de la Roche, M. A., and G. P. Cote. 2001. Regulation of *Dictyostelium* myosin I and II. *Biochim. Biophys. Acta* **1525**:245–261.
- de la Roche, M. A., J. L. Smith, V. Betapudi, T. T. Egelhoff, and G. P. Cote. 2002. Signaling pathways regulating *Dictyostelium* myosin II. *J. Muscle Res. Cell Motil.* **23**:703–718.
- De Lozanne, A., and J. A. Spudich. 1987. Disruption of the *Dictyostelium* myosin heavy chain gene by homologous recombination. *Science* **236**:1086–1091.
- Escalante, R., N. Iranfar, L. Sastre, and W. F. Loomis. 2004. Identification of genes dependent on the MADS box transcription factor SrfA in *Dictyostelium discoideum* development. *Eukaryot. Cell.* **3**:564–566.
- Fincham, V. J., M. James, M. C. Frame, and S. J. Winder. 2000. Active ERK/MAP kinase is targeted to newly forming cell-matrix adhesions by integrin engagement and v-Src. *EMBO J.* **19**:2911–2923.
- Franke, J., M. Faure, L. Wu, A. L. Hall, G. J. Podgorski, and R. H. Kessin. 1991. Cyclic nucleotide phosphodiesterase of *Dictyostelium discoideum* and its glycoprotein inhibitor: structure and expression of their genes. *Dev. Genet.* **12**:104–112.
- Friedl, P. 2004. Preshaping and plasticity: shifting mechanisms of cell migration. *Curr. Opin. Cell Biol.* **16**:14–23.
- Fukui, Y. 1990. Actomyosin organization in mitotic *Dictyostelium* amoebae. *Ann. N. Y. Acad. Sci.* **582**:156–165.
- Funamoto, S., K. Milan, R. Meili, and R. A. Firtel. 2001. Role of phosphatidylinositol 3' kinase and a downstream pleckstrin homology domain-containing protein in controlling chemotaxis in *Dictyostelium*. *J. Cell Biol.* **153**: 795–809.
- Giroux, S., M. Tremblay, D. Bernard, J.-F. Cadrin-Girard, S. Aubry, L. Larouche, S. Rousseau, J. Huot, L. Jeannotte, and J. Charron. 1999. Embryonic death of Mek1-deficient mice reveals a role for this kinase in angiogenesis in the labyrinthine region of the placenta. *Curr. Biol.* **9**:369–372.
- Hazzalin, C. A., and L. C. Mahadevan. 2002. MAPK-regulated transcription: a continuously variable gene switch. *Nat. Rev. Mol. Cell. Biol.* **3**:30–40.
- Holt, M. R., and A. Koffer. 2001. Cell motility: proline-rich proteins promote protrusions. *Trends Cell Biol.* **11**:38–46.
- Huang, C., Z. Rajfur, C. Borchers, M. D. Schaller, and K. Jacobson. 2003. JNK phosphorylates paxillin and regulates cell migration. *Nature* **424**:219–223.
- Iranfar, N., D. Fuller, and W. F. Loomis. 2003. Genome-wide expression analyses of gene regulation during early development of *Dictyostelium discoideum*. *Eukaryot. Cell* **2**:664–670.
- Javelaud, D., J. Laboureau, E. Gabison, F. Verrecchia, and A. Mauviel. 2003. Disruption of basal JNK activity differentially affects key fibroblast functions important for wound healing. *J. Biol. Chem.* **278**:24624–24628.
- Kimmel, A. R., and R. A. Firtel. 2004. Breaking symmetries: regulation of *Dictyostelium* development through chemoattractant and morphogen signal-response. *Curr. Opin. Genet. Dev.* **14**:540–549.
- Kimmel, A. R., and C. A. Parent. 2003. The signal to move: *D. discoideum* go orienting. *Science* **300**:1525–1527.
- Klemke, R. L., S. Cai, A. L. Giannini, P. J. Gallagher, P. de Lanerolle, and D. A. Cheresh. 1997. Regulation of cell motility by mitogen-activated protein kinase. *J. Cell Biol.* **137**:481–482.
- Knecht, D. A., and W. F. Loomis. 1987. Antisense RNA inactivation of myosin heavy chain gene expression in *Dictyostelium discoideum*. *Science* **236**:1081–1086.
- Krause, M., A. S. Sechi, M. Konradt, D. Monner, F. B. Gertler, and J. Wehland. 2000. Fyn-binding protein (Fyb)/SLP-76-associated protein (SLAP), Ena/vasodilator-stimulated phosphoprotein (VASP) proteins and the Arp2/3 complex link T cell receptor (TCR) signaling to the actin cytoskeleton. *J. Cell Biol.* **149**:181–194.
- Ku, H., and K. E. Meier. 2000. Phosphorylation of paxillin via the ERK mitogen-activated protein kinase cascade in EL4 thymoma cells. *J. Biol. Chem.* **275**:11333–11340.
- Kuspa, A., and W. F. Loomis. 1992. Tagging developmental genes in *Dictyostelium* by restriction enzyme-mediated integration of plasmid DNA. *Proc. Natl. Acad. Sci. USA* **89**:8803–8807.
- Li, W. W., G. B. Quinn, N. N. Alexandrov, P. E. Bourne, and I. N. Shindyalov. 2003. A comparative proteomics resource: proteins of *Arabidopsis thaliana*. *Genome Biol.* **4**:R51.
- Ma, H., M. Gamper, C. Parent, and R. A. Firtel. 1997. The *Dictyostelium* MAP kinase kinase DdMEK1 regulates chemotaxis and is essential for chemoattractant-mediated activation of guanylyl cyclase. *EMBO J.* **16**:4317–4332.
- Maeda, M., S. Lu, G. Shaulsky, Y. Miyazaki, H. Kuwayama, Y. Tanaka, A. Kuspa, and W. F. Loomis. 2004. Periodic signaling controlled by an oscillatory circuit that includes protein kinases ERK2 and PKA. *Science* **304**:875–878.
- Matsubayashi, Y., M. Ebisuya, S. Honjoh, and E. Nishida. 2004. ERK activation propagates in epithelial cell sheets and regulates their migration during wound healing. *Curr. Biol.* **14**:731–735.
- Mehdy, M. C., D. Ratner, and R. A. Firtel. 1983. Induction and modulation of cell-type specific gene expression in *Dictyostelium*. *Cell* **32**:763–771.
- Moores, S. L., J. H. Sabry, and J. A. Spudich. 1996. Myosin dynamics in live *Dictyostelium* cells. *Proc. Natl. Acad. Sci. USA* **93**:443–446.
- O'Brien, L. E., K. Tang, E. S. Kats, A. Schultz-Geshwender, J. H. Lipschutz, and K. E. Mostov. 2004. ERKs and MMPs sequentially regulate distinct steps of epithelial tubule development. *Dev. Cell* **7**:21–32.
- Parent, C. A. 2004. Making all the right moves: chemotaxis in neutrophils and *Dictyostelium*. *Curr. Opin. Cell Biol.* **16**:4–13.
- Park, K. C., F. Rivero, R. Meili, S. Lee, F. Apone, and R. A. Firtel. 2004. Rac regulation of chemotaxis and morphogenesis in *Dictyostelium*. *EMBO J.* **23**:4177–4189.
- Pouyssegur, J., and P. Lenormand. 2003. Fidelity and spatio-temporal control in MAP kinase (ERKs) signalling. *Eur. J. Biochem.* **270**:3291–3299.
- Renfranz, P. J., and M. C. Beckerle. 2002. Doing (F/L)PPPs: EVH1 domains and their proline-rich partners in cell polarity and migration. *Curr. Opin. Cell Biol.* **14**:88–103.
- Robinson, D. N., K. D. Girard, E. Octaviani, and E. M. Reichl. 2002. *Dictyostelium* cytokinesis: from molecules to mechanics. *J. Muscle Res. Cell Motil.* **23**:719–727.
- Sharp, L. L., D. A. Schwarz, C. M. Bott, C. J. Marshall, and S. M. Hedrick. 1997. The influence of the MAPK pathway on T cell lineage commitment. *Immunity* **7**:609–618.
- Shaulsky, G., R. Escalante, and W. F. Loomis. 1996. Developmental signal transduction pathways uncovered by genetic suppressors. *Proc. Natl. Acad. Sci. USA* **93**:15260–15265.
- Shaulsky, G., A. Kuspa, and W. F. Loomis. 1995. A multidrug resistance transporter/serine protease gene is required for prestalk specialization in *Dictyostelium*. *Genes Dev.* **9**:1111–1122.

48. **Shaulsky, G., and W. F. Loomis.** 2002. Gene expression patterns in *Dictyostelium* using microarrays. *Protist* **153**:93–98.
49. **Simon, M. N., O. Pelegrini, M. Veron, and R. R. Kay.** 1992. Mutation of protein kinase-A causes heterochronic development of *Dictyostelium*. *Nature* **356**:171–172.
50. **Sobko, A., H. Ma, and R. A. Firtel.** 2002. Regulated SUMOylation and ubiquitination of DdMEK1 is required for proper chemotaxis. *Dev. Cell.* **2**:745–756.
51. **Soderbom, F., C. Anjard, N. Iranfar, D. Fuller, and W. F. Loomis.** 1999. An adenyl cyclase that functions during late development of *Dictyostelium*. *Development* **126**:5463–5471.
52. **Stege, J. T., M. T. Laub, and W. F. Loomis.** 1999. Tip genes act in parallel pathways of early *Dictyostelium* development. *Dev. Genet.* **25**:64–77.
53. **Steimle, P. A., S. Yumura, G. P. Cote, Q. G. Medley, M. V. Polyakov, B. Leppert, and T. T. Egelhoff.** 2001. Recruitment of a myosin heavy chain kinase to actin-rich protrusions in *Dictyostelium*. *Curr. Biol.* **11**:708–713.
54. **Traynor, D., M. Tasaka, I. Takeuchi, and J. Williams.** 1994. Aberrant pattern formation in myosin heavy chain mutants of *Dictyostelium*. *Development* **120**:591–601.
55. **Tsiavaliaris, G., S. Fujita-Becker, R. Batra, D. I. Levitsky, F. J. Kull, M. A. Geeves, and D. J. Manstein.** 2002. Mutations in the relay loop region result in dominant-negative inhibition of myosin II function in *Dictyostelium*. *EMBO Rep.* **3**:1099–1105.
56. **van der Does, C., and R. Tampe.** 2004. How do ABC transporters drive transport? *Biol. Chem.* **385**:927–933.
57. **Van Driessche, N., C. Shaw, M. Katoh, T. Morio, R. Sugang, M. Ibarra, H. Kuwayama, T. Saito, H. Urushihara, M. Maeda, I. Takeuchi, H. Ochiai, W. Eaton, J. Tollett, J. Halter, A. Kuspa, Y. Tanaka, and G. Shaulsky.** 2002. A transcriptional profile of multicellular development in *Dictyostelium discoideum*. *Development* **129**:1543–1552.
58. **Volmat, V., M. Camps, S. Arkinstall, J. Pouyssegur, and P. Lenormand.** 2001. The nucleus, a site for signal termination by sequestration and inactivation of p42/p44 MAP kinases. *J. Cell Sci.* **114**:3433–3443.
59. **Wang, B., and A. Kuspa.** 1997. *Dictyostelium* development in the absence of cAMP. *Science* **277**:251–254.
60. **Webb, D. J., K. Donais, L. A. Whitmore, S. M. Thomas, C. E. Turner, J. T. Parsons, and A. F. Horwitz.** 2004. FAK-Src signalling through paxillin, ERK and MLCK regulates adhesion disassembly. *Nat. Cell Biol.* **6**:154–161.
61. **Wessels, D., and D. R. Soll.** 1998. Computer-assisted characterization of the behavioral defects of cytoskeletal mutants of *Dictyostelium discoideum*, p. 101–140. *In* D. R. Soll and D. Wessels (ed.), *Motion analysis of living cells*. Wiley-Liss, New York, N.Y.
62. **Wessels, D., D. R. Soll, D. Knecht, W. F. Loomis, A. De Lozanne, and J. Spudich.** 1988. Cell motility and chemotaxis in *Dictyostelium* amebae lacking myosin heavy chain. *Dev. Biol.* **128**:164–177.
63. **Wu, L., J. Franke, R. L. Blanton, G. J. Podgorski, and R. H. Kessin.** 1995. The phosphodiesterase secreted by prestalk cells is necessary for *Dictyostelium* morphogenesis. *Dev. Biol.* **167**:1–8.
64. **Yuen, I. S., and R. H. Gomer.** 1994. Cell density-sensing in *Dictyostelium* by means of the accumulation rate, diffusion coefficient and activity threshold of a protein secreted by starved cells. *J. Theor. Biol.* **167**:273–282.
65. **Yujiri, T., M. Ware, C. Widmann, R. Oyer, D. Russell, E. Chan, Y. Zaitso, P. Clarke, K. Tyler, Y. Oka, G. R. Fanger, P. Henson, and G. L. Johnson.** 2000. MEK kinase 1 gene disruption alters cell migration and c-Jun NH2-terminal kinase regulation but does not cause a measurable defect in NF- κ B activation. *Proc. Natl. Acad. Sci. USA* **97**:7272–7277.